Masaki Shirakura
Noritaka Fujii
Hideo Ohnishi
Yuya Taguchi
Hayato Ohshima
Shuichi Nomura
Takeyasu Maeda

Tissue response to titanium implantation in the rat maxilla, with special reference to the effects of surface conditions on bone formation

Authors' affiliations:
Masaki Shirakura, Noritaka Fujii, Hideo Ohnishi, Yuya Taguchi, Hayato Ohshima, Takeyasu Maeda, Division of Oral Anatomy, Department of Oral Biological Science, Niigata University Graduate School of Medical and Dental Sciences, Gakkocho-dori, Niigata, Japan
Masaki Shirakura, Noritaka Fujii, Hideo Ohnishi, Yuya Taguchi, Shuichi Nomura, Division of Oral Health in Aging and Fixed Prosthodontics, Department of Oral Health Science, Niigata University Graduate School of Medical and Dental Sciences, Gakkocho-dori, Niigata Japan
Takeyasu Maeda, Center for Transdisciplinary Research, Niigata University, Gakkocho-dori, Niigata, Japan
Hayato Ohshima, Division of Anatomy and Cell Biology of the Hard Tissue, Department of Tissue Regeneration and Reconstruction, Niigata University Graduate School of Medical and Dental Sciences, Gakkocho-dori, Niigata, Japan

Correspondence to:
Prof. Takeyasu Maeda
Division of Oral Anatomy
Department of Oral Biological Science
Niigata University Graduate School of Medical and Dental Sciences
2-5274 Gakkocho-dori
Niigata 951-8514
Japan
Tel.: +81 25 227 2815
Fax: +81 25 223 6499
e-mail: maedat@dent.niigata-u.ac.jp

Date:
Accepted 19 September 2002

To cite this article:
Shirakura M, Fujii N, Ohnishi H, Taguchi Y, Ohshima H, Nomura S, Maeda T. Tissue response to titanium implantation in the rat maxilla, with special reference to the effects of surface conditions on bone formation. *Clin. Oral Impl. Res.* **14**, 2003; 687–696

Key words: osseointegration, osseogenesis, surface condition, tissue response, titanium implant

Abstract: Tissue responses to titanium implantation with two different surface conditions in our established implantation model in rat maxillae were investigated by light and transmission electron microscopy and by histochemistry for tartrate-resistant acid phosphatase (TRAPase) activity. Here we used two types of implants with different surface qualities: titanium implants sandblasted with Al_2O_3 (SA-group) and implants coated with hydroxyapatite (HA-group). In both groups, bone formation had begun by 5 days postimplantation when the inflammatory reaction had almost disappeared in the prepared bone cavity. In the SA-group, however, the bone formation process in the bone cavity was almost identical to that shown in our previous report using smooth surfaced implants (Futami et al. 2000): new bone formation, which occurred from the pre-existing bone toward the implant, was preceded by active bone resorption in the lateral area with a narrow gap, but not so in the base area with a wide gap. In the HA-group, direct bone formation from the implant toward the pre-existing bone was recognizable in both lateral and base areas. Many TRAPase-reactive cells were found near the implant surface. On the pre-existing bone, new bone formation occurred with bone resorption by typical osteoclasts. Osseointegration around the implants was achieved by postoperative day 28 in both SA- and HA-groups except for the lateral area, where the implant had been installed close to the cavity margin. These findings indicate that ossification around the titanium implants progresses in different patterns, probably dependent on surface properties and quality.

Dental implants in the partially edentulous mouth have been widely accepted as a prosthodontic therapy with a high success rate. Owing to its good prognosis over an extended period, osseointegration has been regarded as the most appropriate bone–implant interface (Adell et al. 1981; Nevins & Langer 1993; Esposito et al. 1998). This osseointegration has been defined as a direct and functional combination at the level of light microscopy (Brånemark et al. 1977, 1985; Albrektsson et al. 1981). To date, many researchers and clinicians have improved the implantation techniques and materials to achieve better osseointegration at the bone–implant interface, and regard the surface quality and properties of implants as one important factor for osseointegration. For instance, porous coated implants have been thought to increase fixation and stability by mechanical interlocking and bone in-growth formation (Puleo & Nanci 1999), while hydroxyapatite(HA)-coating has been judged effective for conducting bone formation due to its high biocompatibility (Gottlander et al.

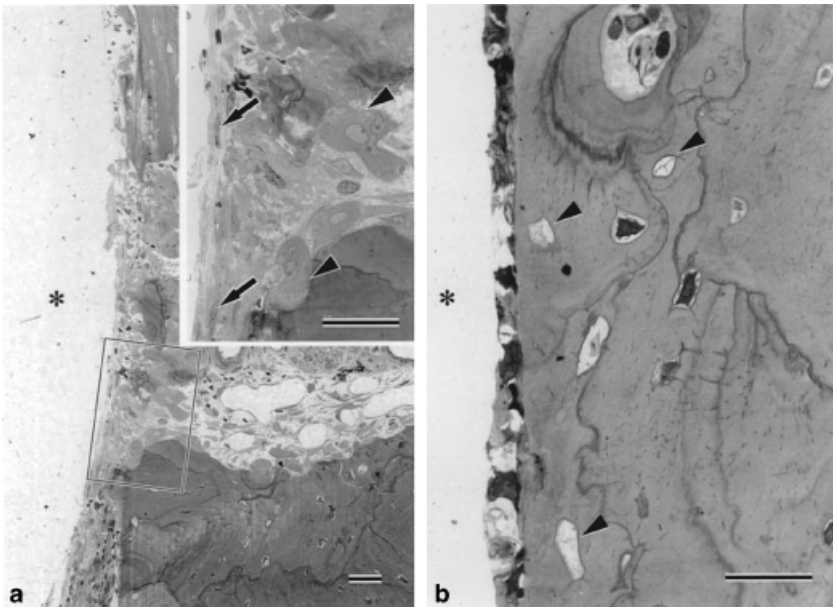

Fig. 1. Cytological views of the lateral areas with a narrow gap (a) and tight contact (b) in the SA-group at 3 days after implantation. Plastic sections stained with toluidine blue. (a) The interface between the pre-existing bone and implant contains various cellular elements. (Inset) Higher magnification of the boxed area in (a). Flat fibroblast-like cells (arrows) are arranged around the implant, and many multinucleated giant cells (arrowheads) are located on the surface of the pre-existing bone. (b) Cell debris and bone fragments are seen on the bone-implant interface. Note the presence of bone lacunae without osteocytes (arrowheads) and with degenerated ones. ∗ denotes implant space. Bars = 25 μm.

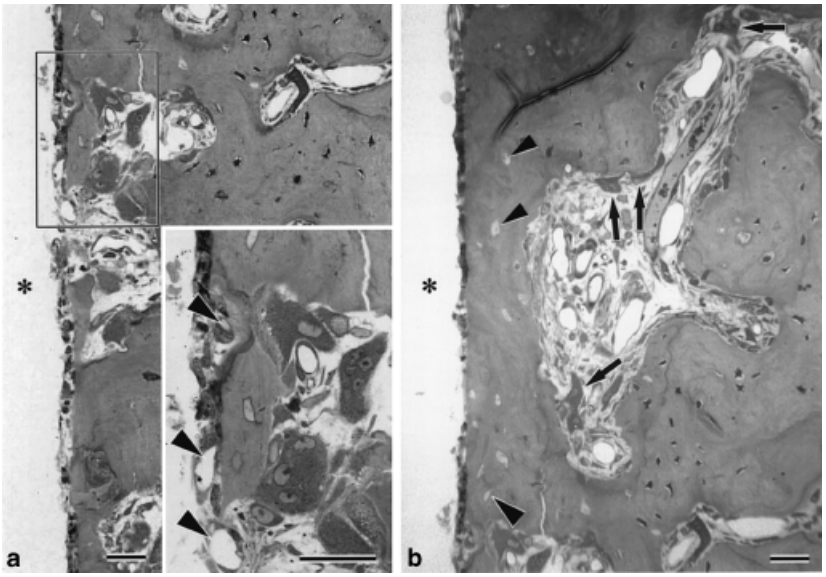

Fig. 2. Light microscopic views of the lateral areas with a narrow gap (a) and tight contact (b) in the HA-group at 3 days after implantation. Plastic sections stained with toluidine blue. (a) The cellular elements occupy the interface between the pre-existing bone and implant. (Inset) Higher magnification of the boxed area in (a) No fibroblast-like cells are present in the bone-implant interface, but blood vessels are located near the implant (arrowheads). (b) Cell debris and bone fragments are seen on the bone–implant interface. Note the presence of empty osteocytic lacunae in the pre-existing bone (arrowheads). ∗ denotes implant space; arrows denotes osteoclasts. Bars = 25 μm.

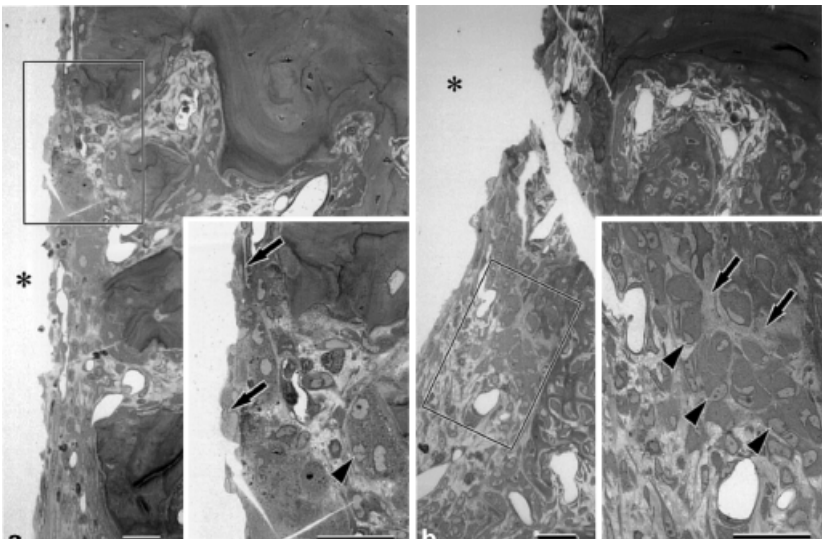

Fig. 3. Light micrographs showing tissue reactions on the lateral (a) and base area (b) in the SA-group at 5 days after implantation. (a) Instead of inflammatory cells, the cellular elements at the bone–implant interface appear to increase in density. (Inset) Higher magnification of the boxed area in (a). Flat fibroblast-like cells (arrows) remain around the implant, and many multinucleated giant cells (arrowheads) are found on the surface of the pre-existing bone. (b) Numerous oval-shaped cells are observed in the base area. (Inset) Higher magnification of the boxed area in (b) Oval-shaped cells possessing a rich cytoplasm (arrowheads) are arranged around the newly-formed osteoid or bone (arrows). ∗ denotes implant space. Bars = 25 μm.

1992; Wie et al. 1998; Strnad et al. 2000). In fact, a histo pathological study suggested different cellular and tissue responses to implants with various surface qualities and properties (Puleo & Nanci 1999).

Recently, our research group has established a titanium implant model in rat maxillae, and demonstrated chronological tissue responses to implantation at the light and electron microscopic levels (Fujii et al. 1998, 2003; Futami et al. 2000). This experimental model is advantageous for realizing complete osseointegration, easy chronological observations, and large sample numbers (Fujii et al. 1998). Using this experimental model, Futami et al. (2000) showed that the tissue reaction pattern to implantation depended on the nature of the recipient bones and the dimension of the gap between the implant and prepared bone cavity. However, since they used custom-made titanium implants with a machined surface, no information is available regarding the tissue reaction to implants with different surface qualities and properties in this model.

The present study was, therefore, undertaken to examine the effects of surface quality and properties on the tissue reaction to titanium implants in the rat maxilla, using light and transmission electron microscopy and histochemistry for tartrate-resistant acid phosphatase (TRAPase) activity, a specific enzyme marker for osteoclasts. We compared two kinds of titanium implants with different surface conditions: those sandblasted with Al_2O_3 and those coated with HA, both representative conditions for clinical dentistry.

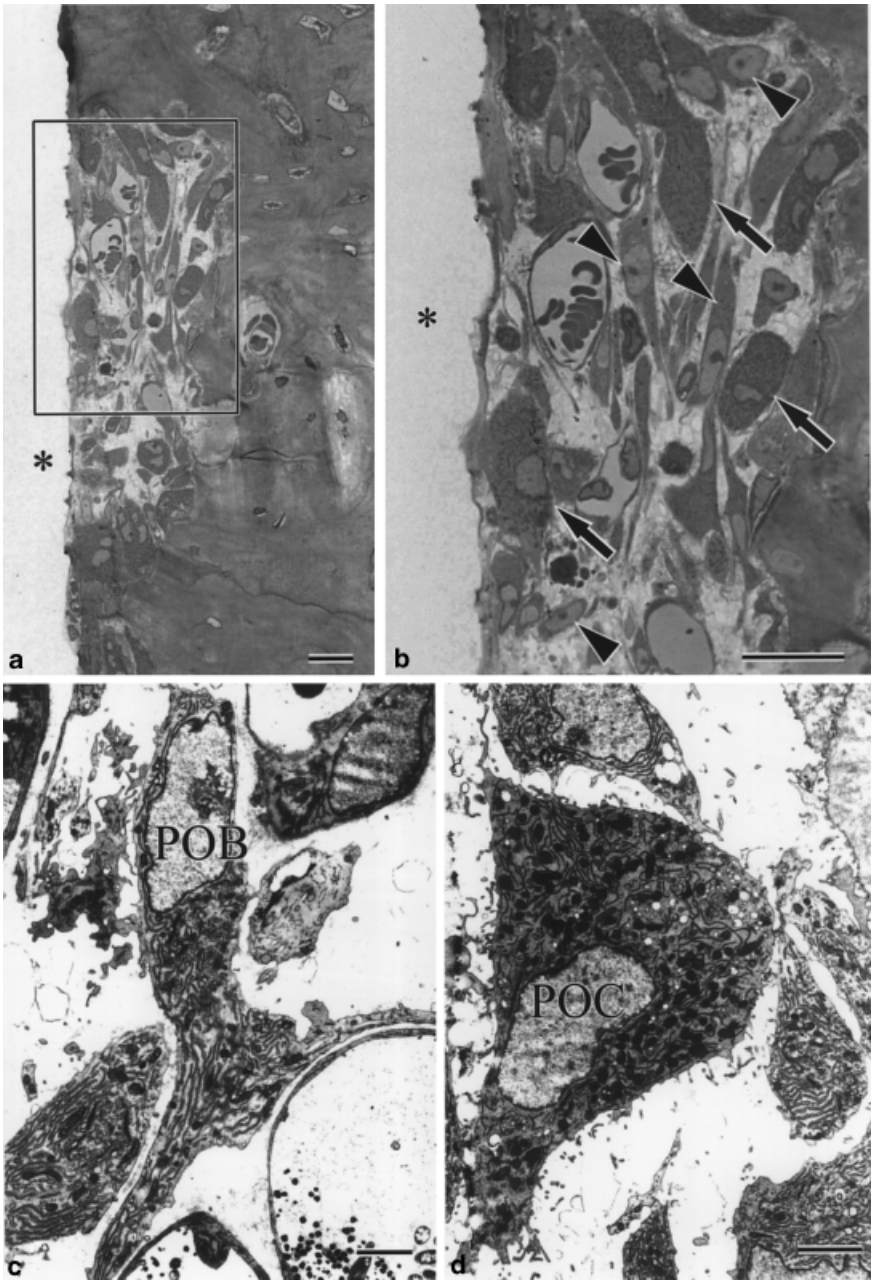

Fig. 4. Light (a, b) and electron micrographs (c, d) of the lateral area in the HA-group at 5 days after implantation. (a) No inflammatory cells are found in the bone–implant interface, and the cellular elements at the interface increase in density. (b) Higher magnification of the boxed area in (**a**). Spindle-shaped cells with clear nucleoli (arrowheads) and giant cells (arrows) are located at the bone–implant interface. (c) Ultrastructure of a preosteoblast (POB) at the implant–tissue interface. It contains well-developed cell organelles such as a rough endoplasmic reticulum and Golgi apparatus. (d) Ultrastructure of a preosteoclast (*POC*). It possesses numerous mitochondria in the cytoplasm. * denotes implant space. Bars = 25 μm (a, b), 2.5 μm (c, d).

Material and methods

All experiments were performed following the Guidelines of the Niigata University Institutional Animal Use and Care Committee.

Animals and experimental procedure

Thirty-six male 4-week-old Wistar rats were used in this experimental study. The implantation protocol has been reported in our previous reports (Fujii et al. 1998; Futami et al. 2000). Briefly, at 1 month after extraction of the upper first molars on both sides (animal age: 8 weeks old), a full-thickness flap was elevated at the recipient sites for implantation under anesthesia by an intraperitoneal injection of 8% chloral hydrate (400 mg/kg, BW). Bone cavities for implantation (1.15 mm in diameter and 3 mm in depth) were prepared by drilling with an engine reamer and a Peeso drill (Maillefer Co. Ltd, Ballaigues, Switzerland). Profuse irrigation with sterilized physiological saline was maintained throughout this process.

In this study, we used two types of custom-made titanium implants with a bullet-shaped base (1.14 mm in diameter, 2.01 mm in length) (Platon Japan Co. Ltd.,

Tokyo, Japan): one sandblasted with Al_2O_3 (diameter 200 μm) and acid-etched (SA-group), and the other coated with HA (HA-group). The SA- and HA-titanium implants were inserted randomly into either the right or left bone cavities by tapping with a mallet (equal numbers of implants between the two groups) so that their bottoms were situated 0.5 mm from the lower cortical bone surface. Then the flaps were repositioned and sutured with silk sutures to cover the implants (i.e. submerged method). After implantation, the animals were housed with free access to water and provided with a powder diet. The animals did not receive any antibiotics.

Histological procedures

Materials were collected at intervals of 1, 3, 5, 7, 14, and 28 days ($n = 6$ each) after implantation. Under deep anesthesia as described above, the animals were perfused transcardially either with the fixative containing 2% paraformaldehyde and 2.5% glutaraldehyde in 0.1 M cacodylate buffer (CB) (pH 7.4) for light and electron microscopy, or cold 4% paraformaldehyde in 0.1 M CB (pH 7.4) for enzyme histochemistry. The maxillae, including the implants, were removed *en bloc*, immersed in the same fixative for an additional 24 h, and decalcified in 5% EDTA-2Na (ethylenediaminetetraacetic acid disodium salt) solution for 4 weeks at 4°C. For histological and histochemical observations, the installed implants were mechanically removed from the bone cavities with forceps according to our previous reports (Ohtsu et al. 1997; Fujii et al. 1998; Futami et al. 2000). Our scanning electron microscopic observations have revealed that this method showed a good preservation of bone–implant interface (Ohtsu et al. 1997; Fujii et al. 1998; Futami et al. 2000). These tissue blocks were dehydrated through an ascending series of ethanol, and embedded in paraffin. Serial sections of the maxillae including the recipient sites were cut frontally at a thickness of 5 μm. For cytological observations, the decalcified tissue blocks with the implants were post-fixed in 1% osmium tetroxide reduced with 1.5% potassium ferrocyanide for 4 h, dehydrated in graded ethanols, and embedded in epoxy resin (Epon 812, Taab, Berkshire, UK). After polymerization, the blocks were frontally ground by an engine-driven bar until exposure of the implant surface, and the block was then cut using a fine saw along a plane through the center line of the implant. The implants were removed from the bone cavities by means of a cryofracture removal technique (James & Schulz 1973; Lausmaa & Linder 1988; Ohtsu et al. 1997; Futami et al. 2000); the plastic embedded blocks were immersed alternately into liquid nitrogen and water. These specimens, freed from the titanium implants, were re-embedded in epoxy resin.

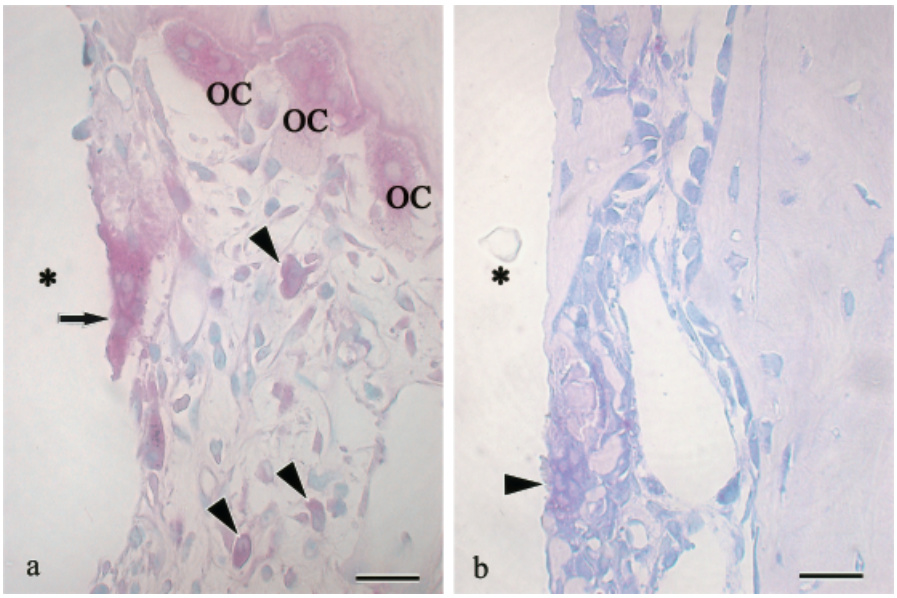

Fig. 5. Histochemistry for tartrate-resistant acid phophatase activity (TRAPase) at the bone–implant interface in the HA-group at 5 (a) and 7 days (b) after implantation. (a) TRAPase-reactions are observed in the osteoclasts (*OC*) and an osteoclast-like cell (arrow) on both the surface of the pre-existing bone and implant at the opening sites of the bone marrow. The presence of TRAPase-reactive mononuclear cells in the intervening layer (arrowheads). (b) TRAPase-reactive multinuclear cells (arrowhead) remain in the perimeter of the implant at the opening area of the bone marrow. * denotes implant space. Bars = 25 μm.

Light and transmission electron microscopy

One-micrometer thick sections were frontally cut from the Epon-embedded blocks and stained with 0.03% toluidine blue. Ultrathin sections, at a thickness of 70 nm, were prepared with an ultramicrotome (Ultracut-R, Leica, Wien, Austria). They were doubly stained with uranyl acetate and lead citrate, and examined under a Hitachi H-7000 transmission electron microscope (Hitachi Co. Ltd. Tokyo, Japan).

Histochemistry for TRAPase activity

Deparaffinized sections were processed for the histochemical demonstration of TRAPase activity by the azo-dye method (Burstone 1961) with slight modifications. The incubation medium comprised 0.06% fast red violet LB salt (Sigma Chemical Co., St Louis, MO, USA), 0.01% naphthol AS-MX phosphate (Sigma Chemical Co.), and 50 mM L-(+)-sodium tartrate in 0.1 M acetate buffer (pH 5.2). The incubation was carried out for 60 min at 37°C. The sections were counterstained with 0.03% methylene blue.

Histological observation

Deparaffinized sections were stained with hematoxylin and eosin, or processed for Azan staining.

Observation area

Since the tissue reactions to implantation have been found to differ between the observation areas in this experimental model (Futami et al. 2000), we selected two portions in this study for examination: the lateral wall and the base part of the

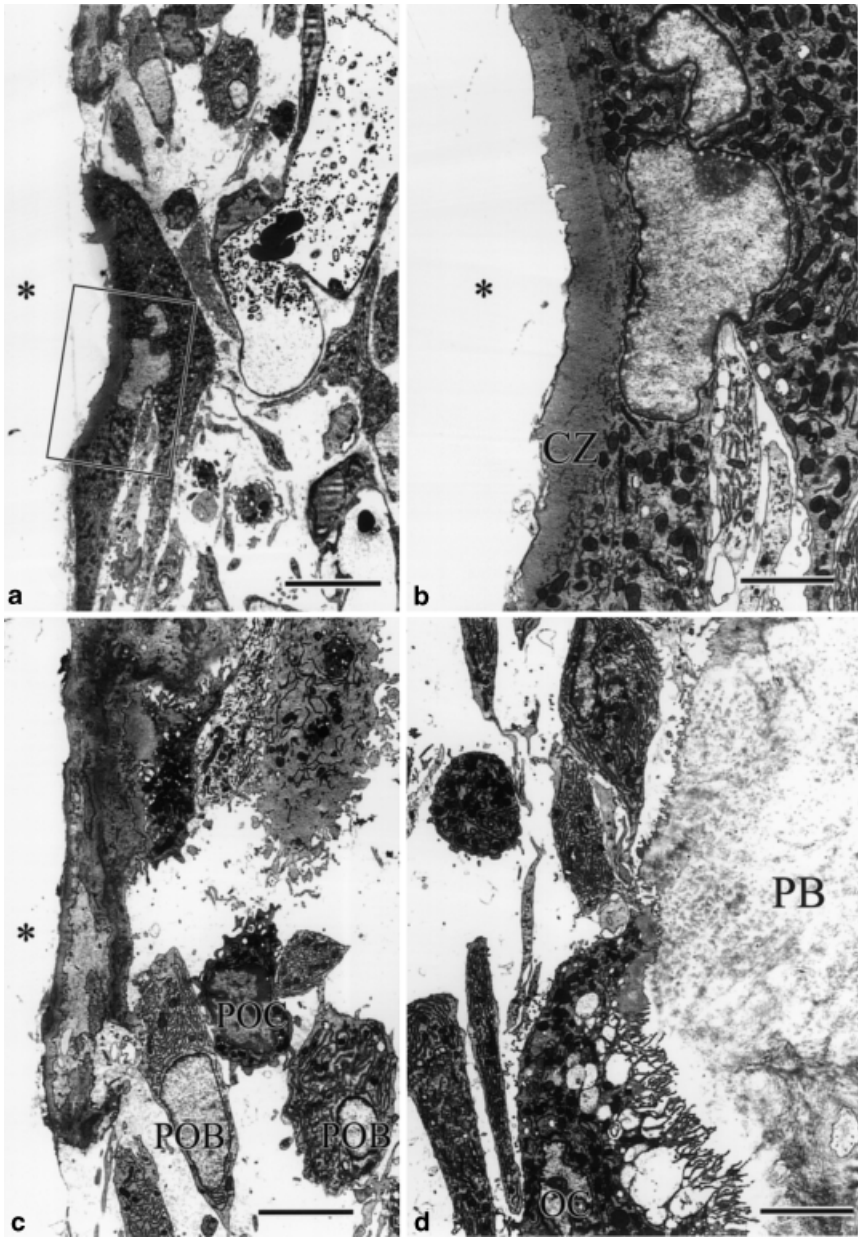

Fig. 6. Electron microscopic views showing the cellular elements in the lateral area in the HA-group at 5 days after implantation. (a) An osteoclast-like cell with numerous mitochondria is situated on the implant surface. (b) Higher magnification of the boxed area in (a) This cell possesses an organella-free clear zone (*CZ*), but no typical ruffled border. (c) In the intervening area, the preosteoclasts (*POC*) and preosteoblast (*POB*) are found near the osteoclast-like cell. They are seen to make contact with each other by their cell processes. (d) Typical osteoclasts with a developed ruffled border appear to resorb the pre-existing bone (*PB*). ∗ denotes implant space. Bars = 10 μm (a), 2.5 μm (b), 5 μm (c, d).

implant cavities, defined as 'lateral' and 'base' areas, respectively. According to Futami et al. (2000), the lateral area was further classified into two portions: the narrow gap and close contact areas. The base area had a wide gap between the implants and the pre-existing bone.

Results

One day after implantation (data not shown)

No difference in tissue responses to titanium implants was recognized between the SA- and HA-groups. The implant surface was either in close contact with the bone cavity in parts of the lateral area, or narrow and wide gaps intervened between them in the lateral and base area, respectively. Many red blood cells, inflammatory cells exclusively consisting of neutrophils, and degenerating cellular elements were observed to concentrate throughout the gaps of both areas. The pre-existing bone contained empty osteocytic lacunae within 100 μm from its surface, these were devoid of any osteocytes or contained pyknotic osteocytes.

Three days after implantation

In both groups, an infiltration of inflammatory cells gradually tended to disappear in the lateral area with narrow gaps, but many red blood cells remained (Figs 1a, 2a). Observation of plastic sections in the SA-group showed that spindle-shaped or flattened cells occurred in the space between the pre-existing bone and implant, and that more flat fibroblast-like cells were arranged around the implant (Fig. 1a). In the HA-group, these fibroblast-like cells were rarely observed in the bone–implant interface in the lateral area with narrow gaps, and blood vessels were located near the implant (Fig. 2a). In both SA- (Fig. 1a) and HA-groups (Fig. 2a), many osteoclasts were located between the pre-existing bone and implant, as well as inside the bone marrow space. Some osteoclasts were present at the surface of the pre-existing bone. In the lateral area with close contacts, on the other hand, cell debris and bone fragments were observed in the bone–implant interface in the area of close contact in both groups (Figs 1b, 2b). The osteocytic lacunae that lacked intact osteocytes remained in the pre-existing bone (Fig. 1b). The base area of both groups contained more cellular elements including many degenerating cells, red blood cells, and spindle-shaped or flattened cells (data not shown).

Five days after implantation

In both groups, inflammatory cells disappeared almost completely by 5 days after implantation (Figs 3, 4), and the cellular elements at the interface of the lateral area with narrow gaps increased in density (Figs 3a, 4a). In particular, a remarkable occurrence of cuboidal or spindle-shaped cells

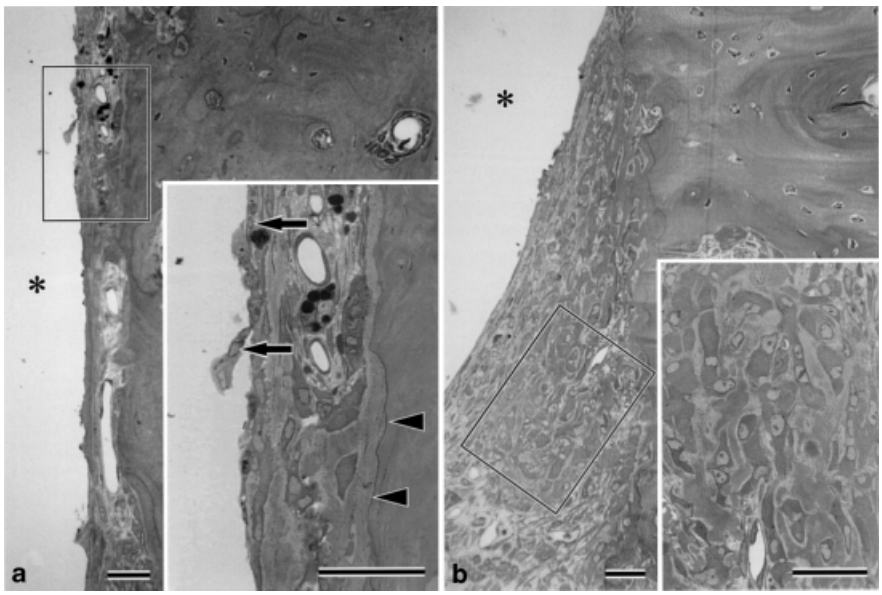

Fig. 7. Light micrographs of the lateral (a) and base area (b) in the SA-group at 7 days after implantation. (a) A few cellular elements remain at the bone-implant interface. (Inset) Higher magnification of the boxed area in (**a**). Flat fibroblast-like cells (arrows) intervene between the implant and the newly formed bone. Note the existence of a clear cement line (arrowheads) intensely stained with toluidine blue between the pre-existing bone and newly formed bone. (b) Bone formation in the base area. (Inset) Higher magnification of the boxed area in (b) Cuboid cells with clear nucleoli are embedded in the bone matrix. ∗ denotes implant space. Bars = 25 μm.

with clear nucleoli and mononuclear giant cells were observed at the bone–implant interface in the HA-group (Fig. 4a, b). The fibroblast-like cells remained on the surface of the pre-existing bone in both cases.

Many osteoclasts were present on the surface of the pre-existing bone at the opening sites of the bone marrow. These cells were intensely reactive to TRAPase activity (Fig. 5a). Furthermore, TRAPase-reactive mononuclear cells were also observed in the intervening layer between the titanium surface and pre-existing bone in the HA-group (Fig. 5a).

Transmission electron microscopic observation demonstrated the ultrastructural features of many cells at the interface between the pre-existing bone and implant on the HA-specimens at this stage. The mononuclear cells were often found at the implant–tissue interface. They had numerous mitochondria, filopodia, and well-developed cell organelles such as a rough endoplasmic reticulum and Golgi apparatus (Fig. 4d), suggesting that they were categorized as preosteoclasts. Osteoclast-like cells that possessed an organella-free clear zone, but lacked a typical ruffled border, were also situated on the implant surface (Fig. 6a, b). In addition to the osteoclast-like cells and preosteoclasts, the mononuclear cells with developed cell organelles including a rough endoplasmic reticulum and Golgi apparatus were present in the intervening area, not on the bone surface; presumably these cells being regarded as preosteoblasts. These presumed preosteoclasts and preosteoblasts frequently contacted each other by their cytoplasmic processes (Figs 4c, 6c). Furthermore, bone resorption by typical osteoclasts with a developed ruffled border was also discernible on the surface of the pre-existing bone (Fig. 6d).

In the base area with wide gaps of the SA-group, on the other hand, oval-shaped cells with an enriched cytoplasm were arranged on the surface of the pre-existing bone where the bone matrix had been formed (Fig. 3b). In the HA-group, the islet-like osteoid was found in the base area, showing that bone formation had also started (data not shown).

Seven days after implantation

Bone formation in both lateral and base areas further proceeded from the pre-existing bone towards the implant surface in the SA-group (Fig. 7a, b), since clear cement lines intensely stained with toluidine blue were distinguishable between the pre-existing bone and newly formed bone. However, since fibroblast-like cells remained on the surface of the implant, the newly formed bone made no contact with the implant (Fig. 7a).

In contrast, bone formation in the HA-group progressed from the implant surface toward the pre-existing bone (Fig. 8a–c), and no cellular elements were laid at the bone–implant interface (Fig. 8c, d). This bone–implant interface appeared rough and showed an irregular surface (Fig. 8d).

TRAP-reactive osteoclasts remained in the perimeter of the implant at the opening area of the bone marrow (Fig. 5b).

Fourteen to 28 days after implantation

In the SA-group, bone formation proceeded throughout the perimeter of the implant, except for the close contact area (Fig. 9a, b). The implants appeared almost surrounded by the newly formed bone, but the interface between the newly formed bone and implant contained a small amount of soft tissue including fibroblast-like cells or blood vessels (Fig. 9a, b).

The HA-group also showed bone formation from the implant surface toward the pre-existing bone, and further exhibited bone formation inside the bone marrow (Fig. 9c). The bone implant interface showed a rugged surface (Fig. 9c). In both groups, complete osseointegration was achieved by 28 days postimplantation.

Discussion

The present study was able to demonstrate clearly the bone formation process in a titanium implantation model using rat maxillae, as established by Fujii et al. (1998) and Futami et al. (2000). Although we used implants with different surface conditions, the present findings are consistent with previous data in that the osseointegration was achieved throughout the implant perimeter by 28 days postimplantation. Since neither a distinct inflammatory reaction nor intervention of a fibrous tissue after the achievement of osseointegration was observed in this study, we confirmed the usefulness of this experimental model for the observation of tissue responses to titanium implantation in jaws.

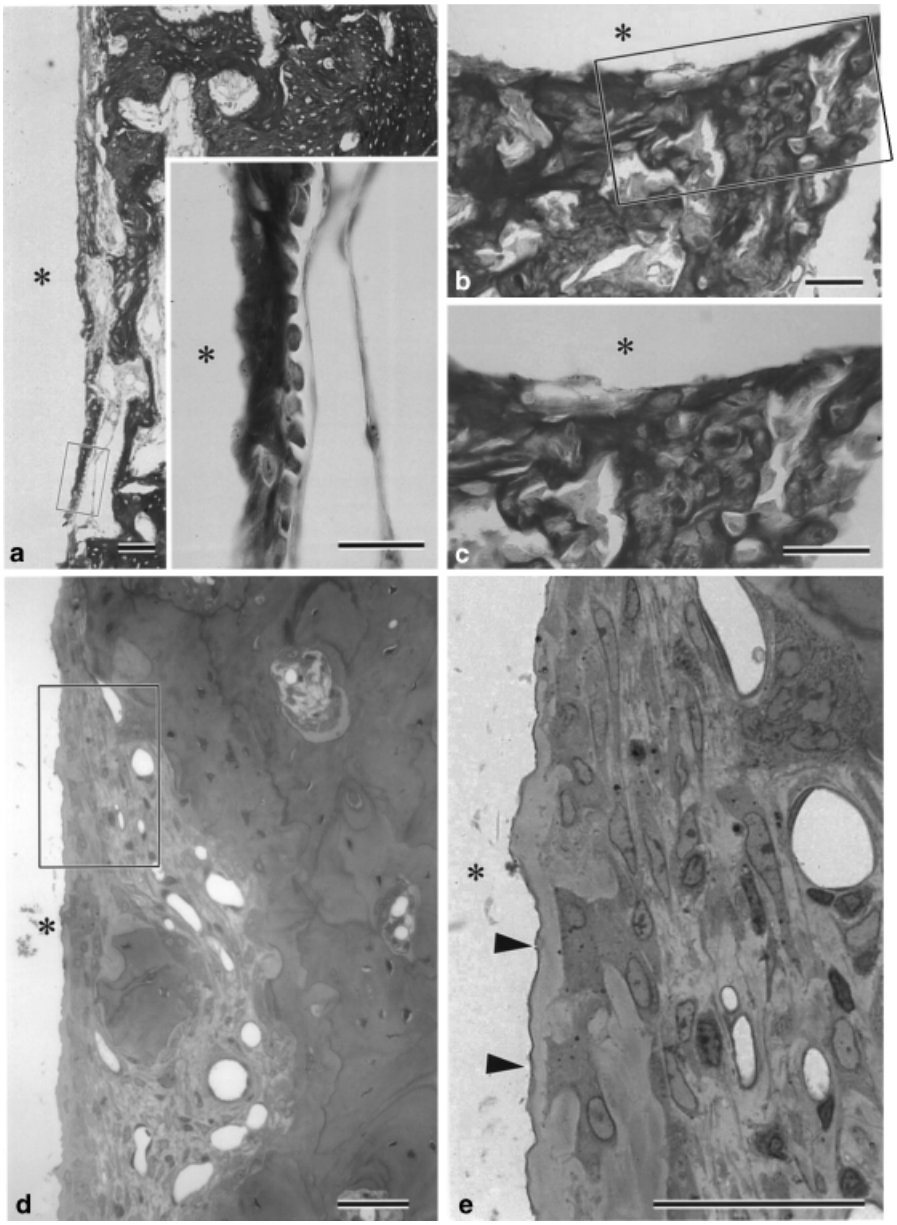

Fig. 8. Light micrographs of the lateral (a, d, e) and base area (b, c) in the HA-group at 7 days after implantation. Paraffin sections with Azan staining (a – c) and plastic sections stained with toluidine blue (d, e). (a) Bone formation proceeds from the implant surface toward the pre-existing bone. (Inset) Higher magnification of the boxed area in (a). Cuboid cells are seen to arrange on the newly formed bone. (b) Bone formation in the base area. The bone matrix occupies the basal area. (c) Higher magnification of the boxed area in (b). Newly formed bone appears to make direct contact with the implant surface. (d) No cellular elements are discernible at the bone–implant interface. (e) Higher magnification of the boxed area in (d) Bone formation proceeds from the implant surface toward the pre-existing bone. Note the rough surface of the bone–implant interface (arrowheads). * denotes implant space. Bars = 100 μm (a), 25 μm (inset, b–e).

The bone formation on the pre-existing bone in the SA-group and at the bone marrow-opening sites in the HA-group occurred from the surface of the pre-existing bone toward the implant with osteoclastic bone resorption. Since bone remodeling is a synchronized phenomenon, in which bone resorption by osteoclasts and bone formation by osteoblasts occur alternately (i.e. the coupling phenomenon) (Farley & Baylink 1982; Baron et al. 1984), the osseointegration in this area requires a cascade of reactions by osteogenic cells. In fact, first multinuclear cells such as osteoclasts appeared, and the bone formation by osteoblasts commenced subsequently.

Tissue responses to implantation have been reported to depend on various factors such as the implant surface, the time at which the sample was evaluated, the recipient sites, and the animal species (Listgarten 1996; Masuda et al. 1998). By comparing findings in implants sandblasted with Al_2O_3 (SA-group; this study) with those in implants with a machined surface (Futami et al. 2000), it was possible to demonstrate the effects of surface quality on the tissue responses to titanium implantation. No difference in tissue responses to implantation, including bone formation around the implants, was recognizable between implants sandblasted with Al_2O_3 and with a machined surface; bone resorption took place on the surface of the pre-existing bone, followed by new bone formation proceeding from this site toward the implant in the lateral area with a narrow gap, whereas no apparent bone resorption was observed in the base areas with a wide gap. In addition, no bone formation was found in the lateral area where the implant had been installed close to the cavity margin. These findings indicate that the surface roughness of the implants does not influence the cellular response and tissue regeneration, including bone formation pattern.

The observation data comparing the Al_2O_3 sandblasted and HA-coated implants showed different directions for bone formation. The HA-coated implants induced bone formation from the implants towards the pre-existing bone, while the direction was opposite in the implants sandblasted with Al_2O_3. The two surfaces have been shown to have different properties, osteoconductivity in the HA-group vs. nonosteoconductivity in the SA-group (Linder et al. 1983, 1989; Kenny et al. 1986; Sapkos et al. 1986; Stahl et al. 1987; Gottlander et al. 1992; Kawaguchi et al. 1992; Sennerby et al. 1993; Clokie & Warshawsky 1995; Fujii et al. 1998; Wie et al. 1998; Futami et al. 2000; Strnad et al. 2000). The difference in the direction of bone formation is plausible, since an intervening soft-tissue layer was observed between the implants and newly formed bone: fibroblast-like cells always appeared in this intervening layer in the SA-group, whereas in the HA-group, soft tissue was found mainly in the form of rich vascularization.

It is noteworthy that osteoclast-like cells reactive to TRAPase activity appeared on

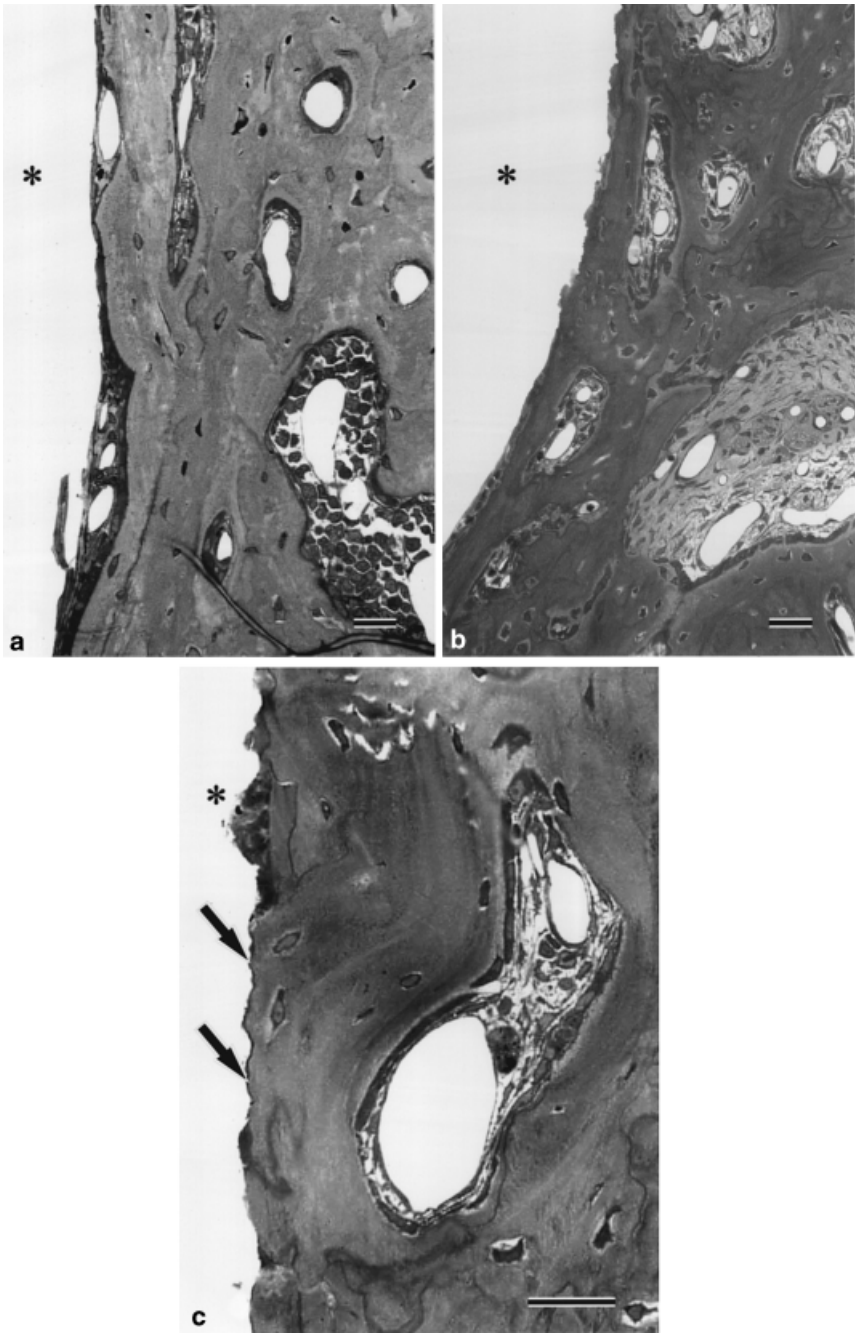

Fig. 9. Light microscopic views of plastic sections with toluidine blue of the lateral (a, c) and base area (b) in the SA-(a, b) and HA-groups (c) at 28 days after implantation. (a) The implants appear to be covered with the newly formed bone, except for an area with a small amount of soft tissue including fibroblast-like cells or blood vessels. (b) The basal area is filled by the newly formed bone on the bone–implant interface. (c) The surface of the pre-existing bone appears rough (arrows). * denotes implant space. Bars = 25 μm (a–c).

the implant surface at postoperative 5 days in the HA-group. They developed an organella-free clear zone, but lacked a typical ruffled border. The occurrence of these cells has been reported in HA implantation into the periodontal tissue on the same postoperative day (Ogilvie et al. 1987; Kawaguchi et al. 1992). In general, bone resorption by osteoclasts with a developed ruffled border is needed prior to new bone formation by osteoblasts; osteoclastic resorption induces the exposure of various kinds of bone matrix substances that modulate the bone surface and accelerate bone formation (Boskey 1989; Butler 1991; Sodek et al. 1991; Young et al. 1992) on the resorptive area. The osteoclastic-like cells observed in this study might only make contact with the HA via a clear zone for recognition of the surface quality. Such a conjecture may be supported by the present findings that the cement-line intensely stained with toluidine-blue was only observed between the pre-existing bone and newly formed bone, and not near the implant surface.

Another interesting finding is the close topographic relationship of osteoclast-like cells with presumed preosteoclasts and preosteoblasts. In this study, the osteoclast-like cells diminished near the implant cells, and instead many osteoblasts appeared by day 7, thereby to deposit bone matrix on the implant surface. Since it has been indicated that osteoblasts play important roles in the differentiation and induction of preosteoclasts by cell-to-cell contact (Matsuzaki et al. 1998; Yasuda et al. 1998), this topographical relation suggests the involvement of preosteoclasts in bone formation.

Acknowledgments: The authors thank the staff of the Division of Oral Anatomy, Niigata University Graduate School of Medical and Dental Sciences, especially Messrs Kiichi Takeuchi and Masaaki Hoshino for their technical assistance. This study was supported by Grants-in-Aid for Exploratory Research (#12557152 to TM) from Japan Society for the Promotion of Science and to promote Multidisciplinary Research from the Ministry of Education, Culture, Sports, Science and Technology.

Résumé

Les réponses tissulaires à l'implantation du titane avec deux conditions de surfaces différentes dans le maxillaire du rat ont été étudiées par microscopie optique et électronique à transmission et par histochimie pour l'activité de l'acide phosphatase résistant au tartrate (TRAPase). Deux types d'implants avec différentes qualité de surface ont été utilisés : des implants en titane sablés par du AL_2O_3 (groupe SA) et des implants couverts par de l'hydroxyapatite (groupe HA). Dans les deux groupes la formation osseuse avait démarré cinq jours après l'implantation, lorsque la réaction inflammatoire avait presque disparue de la cavité osseuse préparée. Cependant, dans le groupe SA le processus de formation osseuse de la cavité osseuse était quasi identique à celle montrée dans un rapport précédent utilisant des implants à surface lisse (Futami *et al.*, 2000) : la néoformation osseuse qui démarre de l'os

préexistant vers l'implant, était précédée par une résorption osseuse active dans l'aire latérale avec une brèche étroite, mais pas dans l'aire de base avec un espace large. Dans le groupe HA, une formation osseuse directe de l'implant vers l'os préexistant était reconnaissable tant dans les aires latérales qu'au niveau de la base. Beaucoup de cellules réactives au TRAPase ont été trouvées près de la surface de l'implant. Sur l'os préexistant une néoformation osseuse est apparue avec une résorption osseuse par des ostéoclastes typiques. L'ostéoïntégration autour des implants a été achevée au jour 28 après l'opération tant dans le groupe SA que HA excepté pour l'aire latérale où l'implant avait été inséré près du rebord de la cavité. Ces découvertes indiquent que l'ossification autour des implants en titane progresse de manière différente dépendant probablement de la qualité et des propriétés de surface.

Zusammenfassung

Die Gewebsantwort auf implantiertes Titan in einem Rattenoberkiefer. Spezielles Augenmerk auf die Einflüsse der Oberflächenbeschaffenheit auf die Knochenbildung.

An unserem etablierten Implantationsmodell am Rattenoberkiefer wurde die Gewebsantwort nach der Titanimplantation von zwei Prüfkörpern mit verschiedener Oberfläche mit Hilfe der Licht- und Transmissionselektronenmikroskopie, sowie mittels Histochemie zum Aktivitätsnachweis der tartratresitenten sauren Phosphatase (TRAPase) untersucht. Wir benutzten hier zwei Implantattypen mit verschiedenen Oberflächen: Mit Al2O3 sandgestrahlte Titanimplantate (SA-Gruppe) und mit Hydroxylapatit beschichtete Implantate (HA-Gruppe). Bei beiden Gruppen begann die Knochenbildung 5 Tage nach der Implantation, sobald die Entzündungsreaktion im präparierten Knochenbett am verschwinden war. In der SA-Gruppe aber, zeigte sich im präparierten Implantatbett ein beinahe gleicher Knochenbildungsvorgang, wie in unseren früheren Berichten für glatte Implantatoberflächen beschrieben (Futami et al., 2000): Die vom bereits vorhandenen Knochen ausgehende Knochenneubildung gegen das Implantat hin erfolgte erst nach einer aktiven Knochenresorption im lateralen Bereich. Es entstand eine minime Spalte zwischen Knochen und Implantat, währenddem im apicalen Bereich eine breitere Spalte entstand. In der HA-Gruppe konnte man sowohl im lateralen, wie auch im apicalen Bereich eine direkt vom Implantat ausgehende Knochenbildung in Richtung des vorhandenen Knochens feststellen. In der Nähe der Implantatoberfläche fand man viele TRAPase-reaktive Zellen. Beim vorhandenen Knochen erfolgte die Knochenneubildung gleichzeitig mit der Knochenresorption durch typische Osteoklasten. Die Osseointegration rund um die Implantate herum erreichte man, ausser im lateralen Bereich gegen den Rand des Implantatbettes hin, in der SA-und der HA-Gruppe am 28igsten postoperativen Tag. Diese Ergebnisse zeigen, dass die Ossifikation um Titanimplantate in verschiedenen Mustern abläuft, wahrscheindlich in Abhängigkeit von der Oberflächeneigenschaft und -qualität.

Resumen

Se investigó las respuestas tisulares a la implantación con titanio con dos condiciones diferentes de superficie en nuestro modelo establecido de implantación en el maxilar de la rata por medio de microscopía óptica y electrónica de transmisión y por medio de histoquímica para la actividad de fosfatasa alcalina tartrato resistente (TRAPase). Hemos usado aquí dos tipos de implantes con diferentes calidades de superficies: Implantes de titanio pulverizados con Al_2O_3 (grupo-SA), e implantes cubiertos con hidroxiapatita (grupo-HA). En ambos grupos la formación de hueso comenzó a los 5 días de la implantación cuando la reacción inflamatoria hubo casi desaparecido en la cavidad ósea preparada. De todos modos, en el grupo SA, el proceso de formación de hueso en la cavidad ósea fue casi idéntico a aquel mostrado en nuestro informe previo usando implantes de superficies lisas (Futami et al., 2000): neoformación de hueso, que tuvo lugar desde el hueso preexistente hacia el implante, siendo precedida por reabsorción ósea activa en el área lateral con un espacio estrecho, pero no así en el área basal con espacio ancho. Se encontraron muchas células TRAPase reactivas cerca de la superficie del implante. En el hueso preexistente, la neoformación ósea tuvo lugar con reabsorción ósea con osteoclastos típicos. La osteointegración alrededor de los implantes se logró al día 28 tras la operación en ambos grupos SA y HA excepto para el área lateral, donde el implante se instaló cerca del margen de la cavidad. Estos hallazgos indican que la osificación alrededor de los implantes de titanio progresa con patrones diferentes, probablemente dependiendo de las propiedades y las calidades de la superficie.

要旨

ラット上顎骨のインプラント埋入モデルにおいて、2つの異なる表面性状を有するチタン製インプラント埋入に対する組織反応を、光学顕微鏡、透過型電子顕微鏡及び酒石酸抵抗性酸性フォスファターゼ（TRAPase）活性の組織化学により調べた。我々は、酸化アルミをサンドブラストしたチタン・インプラント（SA グループ）と、ハイドロキシアパタイトをコーティングしたインプラント（HA グループ）という異なる表面性状を有する2種類のインプラントを用いた。両グループともに、インプラント埋入後5日後、形成した骨窩洞の炎症反応がほぼ消失した時に、骨形成が始まった。しかし SA グループでは、骨窩洞における骨形成の過程は、滑沢な表面のインプラントを用いた我々の過去の研究（Futami et al、2000）で示したものとほとんど同一であった。新生骨の形成は既存骨からインプラントに向かって起こり、それに先立ち狭い空隙のある側方部分に活発な骨吸収が見られたが、広い空隙のある基底部分ではそれほど活発な骨吸収はなかった。HA グループでは側方部分と基底部分の両方において、インプラントから既存骨に向かって直接の骨形成が認められた。多数の TRAPase 陽性細胞がインプラント表面近くに見つかった。既存骨上では、新生骨の形成は典型的な破骨細胞による骨吸収をともなって起った。術後28日後に、インプラントが骨窩洞辺縁近くに埋入された側方部分以外では、SA グループ、HA グループの両方において、インプラント周囲の骨性結合が達成された。これらの所見は、チタン・インプラント周囲の骨性結合は、おそらく表面性状と質によって、異なる様式で進んでゆくという事を示唆している。

キーワード：チタン・インプラント、骨性結合、組織反応、表面性状、骨形成

References

Adell, R., Lekholm, U., Rockler, B. & Brånemark, P.-I. (1981) A 15-year study of osseo-integrated implants in the treatment of the edentulous jaw. *International Journal of Oral Surgery* **10**: 387–416.

Albrektsson, T., Brånemark, P.-I., Hansson, H.A. & Lindstrom, J. (1981) Osseointegrated titanium implants. Requirements for ensuring a long-lasting, direct bone-to-implant anchorage in man. *Acta Orthopaedica Scandinavica* **52**: 155–170.

Baron, R., Vignery, A. & Horowitz, M. (1984) Lymphocytes, macrophages and the regulation of bone remodeling. In: Peck, W.A., ed. *Bone and mineral research*, Annual 2 175–243. New York: Elsevier Science B.V.

Boskey, A.L. (1989) Noncollagenous matrix proteins and their role in mineralization. *Bone and Mineral* **6**: 111–123.

Brånemark, P.-I., Hansson, B.O., Adell, R., Breine, U., Lindstrom, J., Hallen, O. & Ohman, A. (1977) Osseointegrated implants in the treatment of the edentulous jaw. Experience from a 10-year period. *Scandinavian Journal of Plastic and Reconstructive Surgery* **16** (Suppl): 1–132.

Brånemark, P.-I., Zarb, G.A. & Albrektsson, T. (1985) Introduction to osseointegration. In: Brånemark, P.-I., ed. *Tissue-integrated prosthesis. Osseointegration in clinical dentistry*, 11–76. Chicago: Quintessence.

Burstone, M.S. (1961) Histochemical demonstration of acid phosphatases in frozen sections with naphtol AS-phosphates. *Journal of Histochemistry Cytochemistry* **9**: 146–153.

Butler, W.T. (1991) Sialoproteins of bone and dentin. *Journal de Biologie Buccale* **19**: 83–89.

Clokie, C.M. & Warshawsky, H. (1995) Morphologic and radioautographic studies of bone formation in relation to titanium implants using the rat tibia as a model. *International Journal of Oral & Maxillofacial Implants* **10**: 155–165.

Esposito, M., Hirsch, J.M., Lekholm, U. & Thomsen, P. (1998) Biological factors contributing to failures of osseointegrated oral implants. (I). Success criteria and epidemiology. *European Journal of Oral Sciences* **106**: 527–551.

Farley, J.R. & Baylink, D.J. (1982) Purification of a skeletal growth factor from human bone. *Biochemistry/American Chemical Society* **21**: 3502–3507.

Fujii, N., Kusakari, H. & Maeda, T. (1998) A histological study on tissue responses to titanium

implantation in rat maxilla: the process of epithelial regeneration and bone reaction. *Journal of Periodontology* **69**: 485–495.

Fujii, N., Ohnishi, H., Shirakua, M., Nomura, S., Ohshima, H. & Maeda, T. (2003) Regeneration of nerve fibers in the peri-implant epithelium incident to implantation in the rat maxilla as demonstrated by immunocytochemistry for protein gene product 9.5 (PGP 9.5) and calcitonin gene-related peptide (CGRP). *Clinical Oral Implants Research*, **14**: 240–247.

Futami, T., Fujii, N., Ohnishi, H., Taguchi, N., Kusakari, H., Ohshima, H. & Maeda, T. (2000) Tissue response to titanium implants in the rat maxilla: ultrastructural and histochemical observations of the bone-titanium interface. *Journal of Periodontology* **71**: 287–298.

Gottlander, M., Albrektsson, T. & Carlsson, L.V. (1992) A histomorphometric study of unthreaded hydroxyapatite-coated and titanium-coated implants in rabbit bone. *International Journal of Oral & Maxillofacial Implants* **7**: 485–90.

James, R.A. & Schultz, R.L. (1973) Hemidesmosomes and the adhesion of junctional epithelium cells to metal implants. *Journal of Oral Implantology* **4**: 294–302.

Kawaguchi, H., Ogawa, T., Shirakawa, M., Okamoto, H. & Akisaka, T. (1992) Ultrastructural and ultracyto-chemical characteristics of multinucleated cells after hydroxyapatite implantation into rat periodontal tissue. *Journal of Periodontal Research* **27**: 48–54.

Kenney, E.B., Lekovic, V, Sa Ferreira, J.C., Han, T., Dimitrijevic, B. & Carranza, F.A. Jr (1986) Bone formation within porous hydroxyapatite implants in human periodontal defects. *Journal of Periodontology* **57**: 76–83.

Lausmaa, J. & Linder, L. (1988) Surface spectroscopic characterization of titanium implants after separation from plastic-embedded tissue. *Biomaterials/Biological Engineering Society* **9**: 177–280.

Linder, L., Albrektsson, T., Brånemark, P.-I., Hansson, H.A., Ivarsson, B., Jonsson, U. & Lundstrom, I. (1983) Electron microscopic analysis of the bone–titanium interface. *Acta Orthopaedica Scandinavica* **54**: 45–52.

Linder, L., Obrant, K. & Boivin, G. (1989) Osseointegration of metallic implants. II. Transmission electron microscopy in the rabbit. *Acta Orthopaedica Scandinavica* **60**: 135–139.

Listgarten, M.A. (1996) Soft and hard tissue response to endosseous dental implants. *Anatomical Record* **245**: 410–425.

Masuda, T., Yliheikkila, P.K., Felton, D.A. & Cooper, L.F. (1998) Generalizations regarding the process and phenomenon of osseointegration. Part I. *In vivo* studies. *International Journal of Oral & Maxillofacial Implants* **13**: 17–29.

Matsuzaki, K., Udagawa, N., Takahashi, N., Yamaguchi, K., Yasuda, H., Shima, N., Morinaga, T., Toyama, Y., Yabe, Y., Higashio, K. & Suda, T. (1998) Osteoclast differentiation factor (ODF) induces osteoclast-like cell formation in human peripheral blood mononuclear cell cultures. *Biochemical and Biophysical Research Communications* **246**: 199–204.

Nevins, M. & Langer, B. (1993) The successful application of osseointegrated implants to the posterior jaw: a long-term retrospective study. *International Journal of Oral & Maxillofacial Implants* **8**: 428–432.

Ogilvie, A., Frank, R.M., Benque, E.P., Gineste, M., Heughebaert, M. & Hemmerle, J. (1987) The biocompatibility of hydroxyapatite implanted in the human periodontium. *The Journal of Periodontal Research* **22**: 270–283.

Ohtsu, A., Kusakari, H., Maeda, T. & Takano, Y. (1997) A histological investigation on tissue response to titanium-implantation in cortical bone of the rat femur. *Journal of Periodontology* **68**: 270–283.

Puleo, D.A. & Nanci, A. (1999) Understanding and controlling the bone-implant interface. *Biomaterials/Biological Engineering Society* **20**: 2311–2321.

Sapkos, S.W. (1986) The use of Periograf in periodontal defects. Histologic findings. *Journal of Periodontology* **57**: 7–13.

Sennerby, L., Thomsen, P. & Ericson, L.E. (1993) Early tissue response to titanium implants inserted in rabbit cortical bone. Part II. Ultrastructural observation. *Journal of Materials Science – Materials in Medicine* **4**: 494–502.

Sodek, J., Zang, Q., Goldberg, H.A., Domenicucci, C., Kasugai, S., Wrana, J.L., Shapiro, H. & Chen, J. (1991) Noncollagenous bone proteins and their role in substrate-induced bioactivity. In: Davies, JE., ed. *The bone–biomaterial interface*, 97–110. Toronto: University of Toronto Press.

Stahl, S.S. & Froum, S.J. (1987) Histologic and clinical responses to porous hydroxyapatite implants in human periodontal defects. Three to twelve months postimplantation. *Journal of Periodontology* **58**: 689–695.

Strnad, Z., Strnad, J., Povysil, C. & Urban, K. (2000) Effect of plasma-sprayed hydroxyapatite coating on the osteoconductivity of commercially pure titanium implants. *International Journal of Oral & Maxillofacial Implants* **15**: 483–90.

Yasuda, H., Shima, N., Nakagawa, N., Yamaguchi, K., Kinosaki, M., Mochizuki, S., Tomoyasu, A., Yano, K., Goto, M., Murakami, A., Tsuda, E., Morinaga, T., Higashio, K., Udagawa, N., Takahashi, N. & Suda, T. (1998) Osteoclast differentiation factor is a ligand for osteoprotegerin/osteoclastogenesis-inhibitory factor and is identical to TRANCE/RANKL. *Proceedings of the National Academy of Sciences of the United States of America* **95**: 3597–3602.

Young, M.F., Kerr, J.M., Ibaraki, K., Heegaard, A.M. & Robey, P.G. (1992) Structure, expression, and regulation of the major noncollagenous matrix proteins of bone. *Clinical Orthopaedics and Related Research* **281**: 275–294.

Wie, H., Hero, H. & Solheim, T. (1998) Hot isostatic pressing-processed hydroxyapatite-coated titanium implants: light microscopic and scanning electron microscopy investigations. *International Journal of Oral & Maxillofacial Implants* **13**: 837–844.